2020年3月31日

報告書

実施期間 2019年7月8日～2020年3月31日

容量低下バッテリーの再生技術に関する共同研究

“FM Lab” Co Ltd

Daniil Itkis

日産自動車（株）

総合研究所　先端材料・プロセス研究所

中村雅紀、菱谷佳子、戸田貴子

概要

名称

容量低下バッテリーの再生技術に関する共同研究

実施期間

2019年7月8日～2020年3月31日

開発/調査 代表者

“FM Lab” Co Ltd
Daniil Itkis

実施者

“FM Lab” Co Ltd
Daniil Itkis

“SC-Tek” LLC
Dr. Mikhail Kondratenko

日産自動車株式会社　総合研究所　先端材料・プロセス研究所
主管研究員　中村雅紀、主査　菱谷佳子、戸田貴子

目的

使用済み自動車より回収された容量低下したリチウムイオンバッテリーを再生し、定置用電源または自動車用電源としてリサイクルをする為に必要な高度リサイクル技術について研究を行う。

実施内容

本研究では、リサイクル費用の低減に向け、容量低下バッテリーを非破壊で再生する手法開発として、本年度（FY19）FM-Lab では、①文献値から回復率理論値試算、②SEI除去（負極）、③Li補充の方策の有効性について検討し、④劣化セルを用いて方策の効果を確認した。

成果

① 文献値から容量低下因子とその割合を求め、 Li 補充で初期値の約 90%まで戻ることを試算した。
② CO_2超臨界流体にアセトニトリル (ACN)と電解液を添加することで、 SEI を効率的に除去することが可能であることを明らかにした。
③ Li 補充塩としては、と硝酸リチウム ($LiNO_3$) が有効であることを示した。
④ 2 つの方策を実施し、セル (FM-Lab 試作) で、初期値の 90%まで戻ることを確認した。課題は再現性である。

28th February 2020

Final Report

Research period: 8th July 2019 to 31st March 2020

Title:

“Searching the Approaches for Lithium-Ion Battery (LIB) Second Life Performance Improvement”

“FM Lab” Co Ltd

Daniil Itkis

Summary

Title

Searching the Approaches for Lithium-ion Battery (LIB) Second Life Performance Improvement

Research period

8th July 2019 to 31st March 2020

Delegate of the research

“FM Lab”Co Ltd　Name of delegate: Dr. Daniil Itkis

Prosecutor

Company: Nissan Motor Co., Ltd.　Name of prosecutor: Mr. Masanori Nakamura

Subcontractor/delegate

Company: “SC-Tek” LLC　　Name of delegate: Dr. Mikhail Kondratenko

Purpose

The main aim of the project is to monitor and to evaluate promising approaches, which can enable enhancement of the LIB performance during its second life (i.e. approaches enabling recovery of battery capacity and/or power after it was used for some time and has been degraded).

Project Tasks

Task 1. Confirmation of Battery capacity improvement effect by supercritical fluids and Explanation of major influencing factors. Expected Theoretical Improvement ratio calculation

- 1.1 Additional studies of electrolyte extraction and SEI removal from negative electrodes
- 1.2 Studies of the electrolytes for lithium inventory refilling
- 1.3 Testing graphite electrode lithiation from selected “refilling” electrolytes

Task 2. Present the actual proof data (Performance Improvement) and Improvement mechanism (Verification of Theoretical improvement value）

    - 2.1 Testing of battery components stability in supercritical fluids (separator, cathode material, current collectors, binders, carbon additives)
    - 2.2 Testing of battery performance improvement of full 2032 cells
    - 2.3 Testing of battery performance improvement of full pouch cells

Task 3. Proposal on Possible approaches for All-Solid-State Battery regeneration
Task 4. Final report preparation

Summary

An experimental verification of the two-stage approach for improving the properties of spent LIBs suggested at the previous project stage was performed. The ability of full removal of electrolyte from the cells and partial removal of SEI was demonstrated. Pouch cells were found to be fully operational after treatment in supercritical fluids. The candidate “recovery” electrolytes were tested, and unfortunately, only lithium nitrate was found to have enough solubility. Further challenges are identified.

Contents

Abbreviations

ASSB	all-solid-state battery
BPR	back-pressure regulator
CC	constant current
CV	constant voltage
CVA	cyclic voltammetry
DMC	dimethyl carbonate
EC	ethylene carbonate
EIS	electrochemical impedance spectroscopy
ICP MS	inductively coupled plasma mass spectroscopy
LAM	loss of active materials
LIB	lithium-ion battery
LLI	loss of lithium inventory
MeCN	acetonitrile
NMC	Lithium-nickel-manganese-cobalt oxide ($Li(Ni, Mn, Co)O_2$)
NMP	N-methyl-2-pyrrolidone
PVDF	polyvinylidene difluoride
$scCO_2$	supercritical carbon dioxide
SCF	supercritical fluid
SEI	solid-electrolyte interphase
SEM	scanning electron microscopy
TBAP	tetrabutylammonium perchlorate

Introduction

Today the market of electric vehicles actively develops increasing the demand for LIBs. According to various estimates [1,2], the annual amount of LIB waste is *ca.* 200-500 million tons, of which 5-15% belong to cobalt - an expensive and toxic element. Due to expected even more rapid growth of LIB production the battery recycling [1 – 4] and "second life" became quite hot topics driven by both economic and environmental factors. Although battery recycling is rather cost- and labour-consuming, increasing amount of spent batteries pushes active investments into this field. Reusing spent batteries in the applications not requiring high performance – battery "second life" – is on the contrary much less expensive. However, there are serious limitations on energy and power of the spent batteries so the number of applications is quite limited.

In this project we aimed at improving the performance of the spent lithium-ion batteries, to make it possible to use recovered ones during its "second life" in demanding applications such as electric vehicles. Although recovery of initial properties of the new battery seems to be impossible, we believe that the battery capacity and/or peak power can be partially restored. The main aim of the project is evaluating the approach, which was suggested at the previous project stage for enhancement of the LIB performance during its second life.

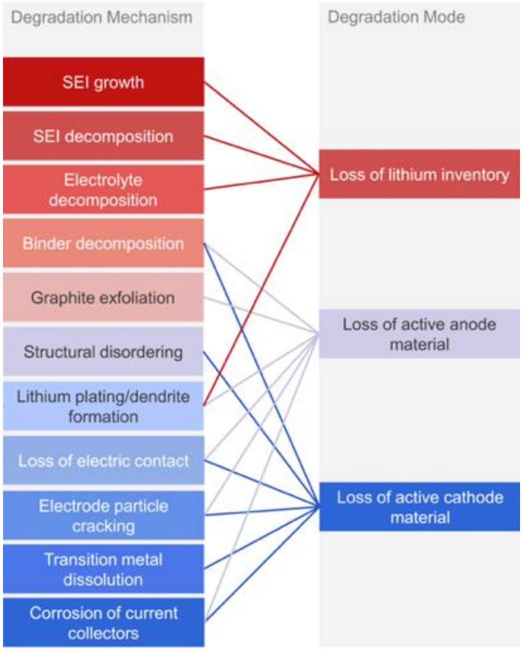

Figure 1 The mechanistic reasons (chemical/electrochemical processes occurring inside the battery during its cycling) and the consequences (modes of degradation) [5].

There are a number of reasons for the loss of battery capacity and power during its discharge/recharge cycling [5] (see Figure 1). At the previous project stage, we supposed that one of the most serious and universal (can be found in majority of LIBs, which have graphite negative electrode) reasons for degradation is damaging of initial SEI (solid-electrolyte interphase) layer and its re-formation leading to active lithium inventory loss. SEI films form on the surface of the negative electrode from the products of electrolyte reduction and decomposition. During the cycling of the battery SEI can be damaged, and a new protective layer is formed. SEI comprise not only organic products of electrolyte solvent reduction but also inorganic part, which include lithium-containing compounds such as Li_2O, LiF, Li_2CO_3. Thus, lithium is partially immobilised in SEI, thus the number of active charge carriers in the cell decreases and the capacity fades. As well, excessive SEI increases the negative electrode resistance thus lowering the cell power characteristics. In addition to lithium inventory loss, there are also another type of degradation – loss of active materials (cathode or anode).

During the current project the paper was published [6], which experimentally demonstrated that lithium inventory loss in fact makes the major contribution to the capacity loss as we expected. By analysing 30 Ah degraded pouch cell it was shown that LLI gives ca. 18.3%, LAM at cathode – 11.4%, while the loss on anode material is quite low 1.8% (see Figure 2).

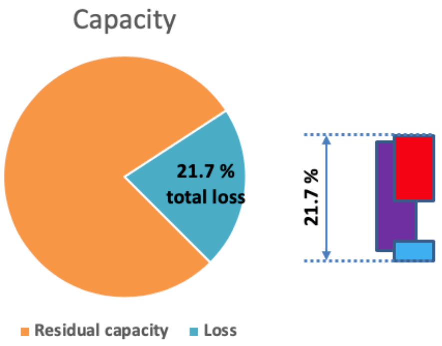

Figure 2 Diagram showing the breakdown of capacity loss for aged 30 Ah pouch cell. The total loss is a superposition (not a sum) of contributions from different degradation modes (LLI in violet (18.3%), LAM at cathode in red (11.4%), LAM at anode in blue (1.8%)) [6].

We proposed an idea for restoring the spent battery capacity, based primarily on removing the SEI layer from the surface of the negative electrode and further "refilling" of lithium inventory in the cell. The general idea is illustrated in Figure 3, which shows partial immobilization of lithium ions in SEI during battery life, removal of old SEI, refilling the lithium inventory using special "recovery" electrolytes and reformation of SEI (lithium oxalate additive to prepare "recovery" electrolyte is shown as an example).

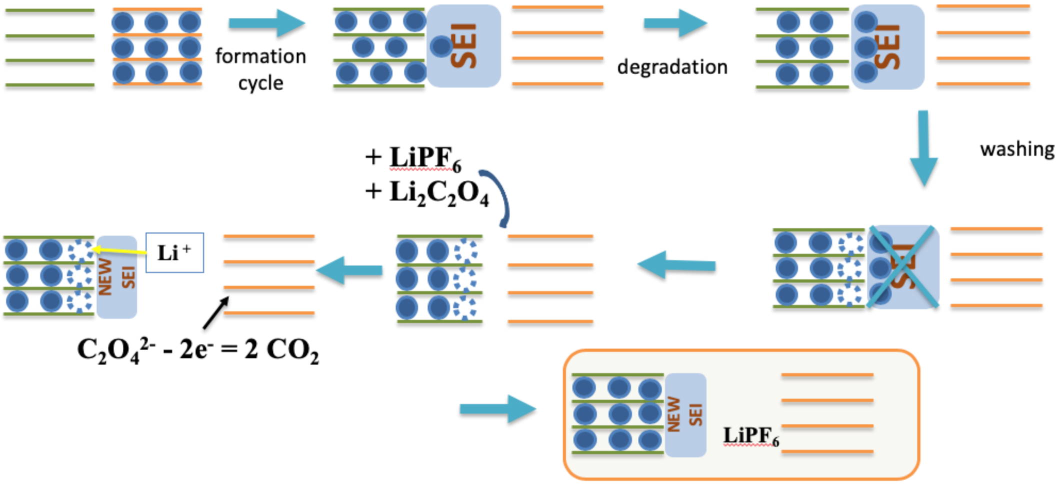

Figure 3 Schematic illustration of the project general idea. Lithium host materials are shown as green (anode) and orange (cathode) layers. Dark blue circles are lithium ions. Dotted circumflexes denote potential host sites for lithium, which are not filled.

At the previous stage we showed the potential ability of removing SEI and old electrolyte from the electrodes or cells by supercritical fluids. During this project stage we further investigated removal of electrolyte and SEI from the cells by dissolution with supercritical fluids (sc-CO_2) and co-solvents (MeCN, EC:DMC) and tested the salts for preparation of “recovery” electrolyte for lithium inventory refilling.

Figure 4 Scheme showing the potential capacity improvement due to lithium inventory refilling.

The methodology of experimental studies

Washing at high pressures

Washing of the electrolytes and the cells was carried using the experimental setup shown in Figure 5. CO_2 pressure was 300 bar, thermostat temperature 60 °C, gas flow 2 ml/min. Each experiment consisted of three steps: 1) preliminary washing of the system with water, 2) washing the sample (battery components or the whole battery) with supercritical carbon dioxide with a co-solvent, 3) final washing of the system with water.

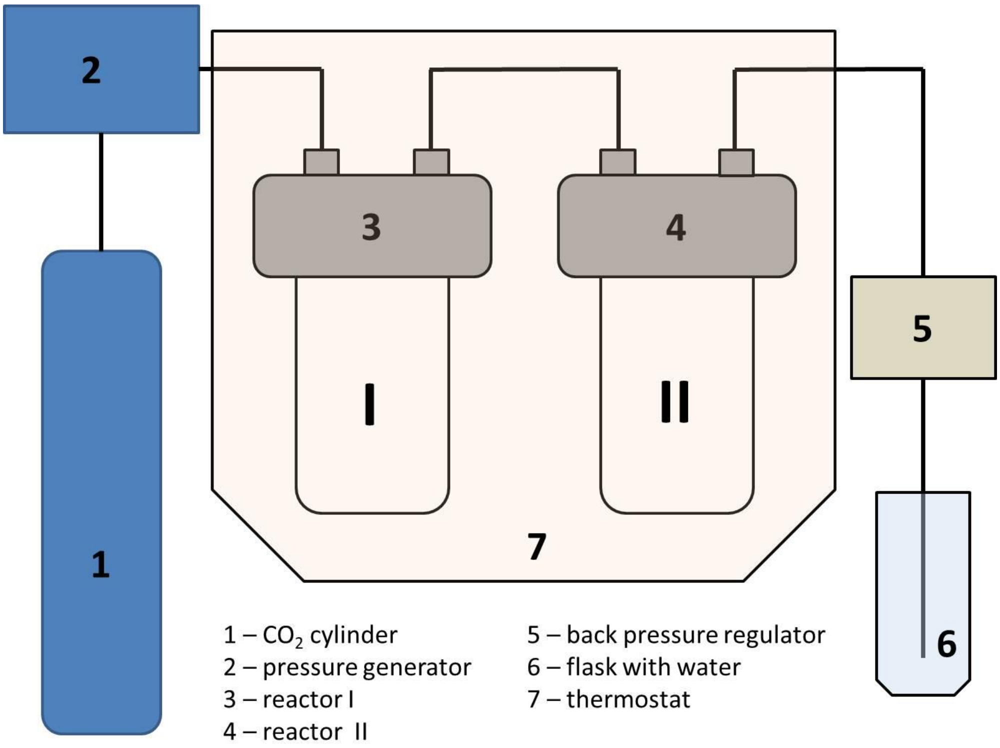

Figure 5. Scheme of the setup for supercritical extraction.

Mass spectroscopy with inductively coupled plasma

The samples were analysed using Perkin Elmer ELAN DRC II spectrometer. The calibration was performed using the samples prepared of lithium ion concentration standards (EcoAnalytica company, Russia). 4 standard samples with concentrations in range 0.1 – 10 mg/l were used for calibration each time.

Preparation of the electrodes and cell assembly

We used the graphite negative electrodes both prepared in-house and from commercial pouch cells. For fabrication of the electrodes we prepared the electrode slurry consiting

95 mass. % of natural graphite (Gelon) and 5 mass. % of PVDF binder (Solvay Solef 5130). For slurry preparation 0.9 g of PVDF was mixed with 12ml NMP (BASF, battery grade) and stirred for 3 hours. After that, 17.1 g of graphite was added to the polymer solution, the mixture was sonicated to disaggregate large graphite agglomerates and then it was stirred by high-shear mixer with a dissolver stirrer for 15 hours. The density of the obtained slurry was 1.5 g/ml. The slurry was casted onto the copper foil (20 μm, Gelon) using automatic film applicator coater (Zehntner ZAA 2300) operating at a coating speed of 20 mm/s. Wet coating thickness was set to be 100, 200, 300 or 400 μm. The electrodes were dried in air at 80°C shrinking by about two times. Prepared electrodes were calandered using hot rolling press (MTI corp.) at 80°C. The initial dry thickness of the coating (excluding the foil thickness) was compressed by 5, 10 or 15%. Further, the electrodes were cut into 15 mm diameter discs, dried at 105°C in vacuum for 12 hours and transferred to glove box without exposition to air.

Coin cells battery were assembled inside an argon-filled glove box with oxygen and water content below 5 and 0.1 ppm, respectively. The graphite electrodes played a role of working electrode, metallic lithium served as a counter electrode (Li discs, 110 μm thickness, China Energy Lithium). The electrodes were separated by a single-layer polypropylene separator (Celgard 2500). 1 M $LiPF_6$ in EC:DMC 1:1 (vol.) (Sigma-Aldrich) served as an electrolyte.

Glass three-electrode cells were used for CVA. Metallic lithium was used as a reference electrode, Pt wire – as a counter electrode.

Electrochemical measurements

The graphite electrodes were analysed in galvanostatic charge-discharge experiments. Lower voltage cut-off was set to 5 mV. All measurements of coin and pouch cells were carried out using Biologic SAS MPG-2 multichannel potentiostat. Measurements of three-electrode electrochemical cells were carried out with Biologic SAS SP-300 potentiostat with frequency response analyser for EIS meaurements.

Electrodes characterization

Micrographs were obtained using Carl Zeiss Supra 50 VP microscope equipped with Oxford instruments INCA Energy+ EDX spectrometer.

Results

Washing the cell components and batteries by supercritical fluids

At the previous project stage, we showed that $scCO_2$ can effectively wash out the aprotic solvents from the electrodes, while addition of co-solvent to supercritical fluid helps in washing ionic compounds, namely $LiPF_6$. At the same time, it was required to ensure that electrode materials are not damaged by such a treatment. While the stability of oxide or phosphate materials was not under question, we checked the stability of graphite, which might be delaminated in such condition. The microstructure of the electrode upon treatment by $scCO_2$ at 200 bar was monitored by SEM (see Figure 6).

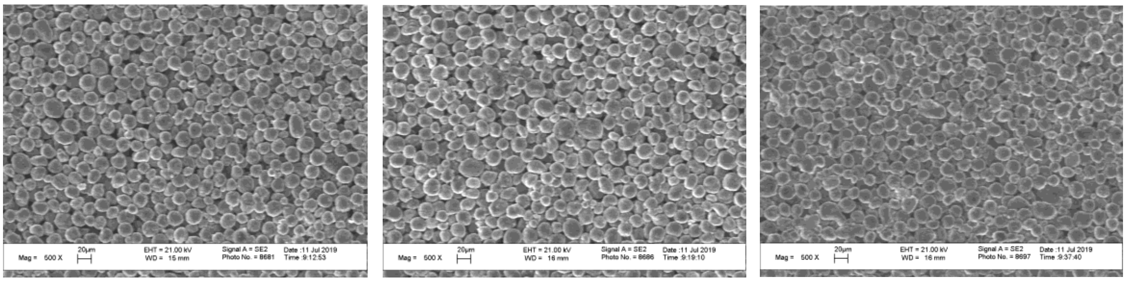

Figure 6 SEM micrographs of the pristine graphite LIB electrode, the electrode after treatment by $scCO_2$ at 200 bar, and after soaking in 1M LiPF6 solution in EC:DMC mixture and further treatment by $scCO_2$ (left to right).

No significant changes of the surface morphology were found to happen after treatment of the electrode by $scCO_2$. To quantitively analyze the possible damage to spheroidized natural graphite particles we checked the particle size distributions and found no changes as seen in Figure 7.

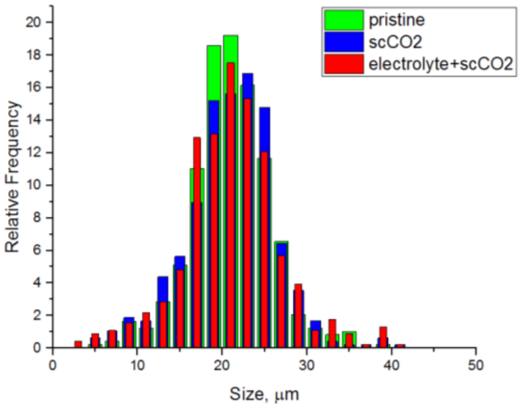

Figure 7 Graphite particle size distribution obtained from statistical analysis of SEM micrographs.

The microstructure of the electrode upon treatment by $scCO_2$ at higher pressure (up to 500 bar) and with addition of co-solvent (acetonitrile) was also monitored by SEM. As for the case of treatment at 200 bar, no significant changes of the surface morphology were found to happen, particle size distributions changed neither.

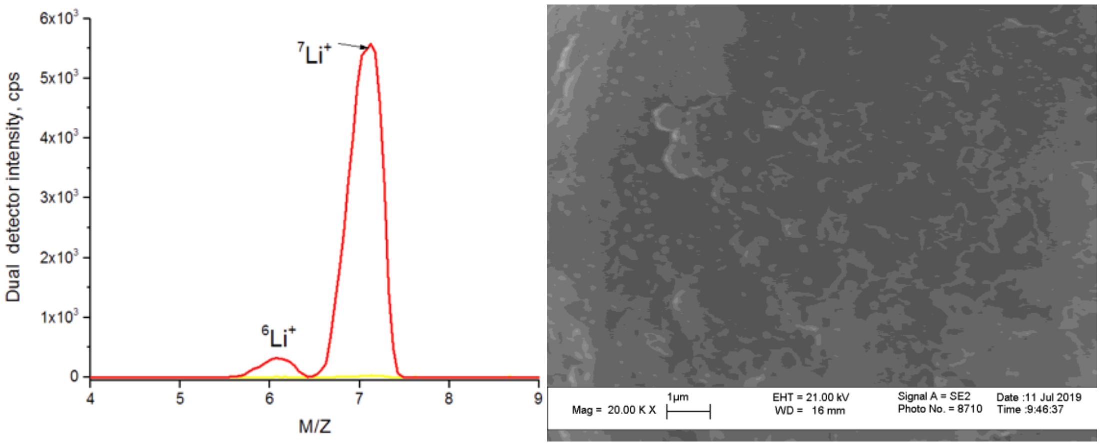

Figure 8 Left – mass spectrum of the probe collected at the exhaust of high-pressure system during washing of the graphite electrode with formed SEI. Right – SEM micrograph of the graphite particle surface. The electrode was kept in the electrolyte, and then washed by $scCO_2$ for 2 hours.

Although the spectral signature of lithium, washed out from the adsorbed electrolyte (and probable SEI layer on graphite) was found in ICP MS data (see Figure 8, left), probably not all lithium containing products are extracted. It was found that the electrodes soaked with electrolyte (1M $LiPF_6$ in EC:DMC) contained small (ca. 100 nm) particles on the surface of graphite, which can be seen in Figure 8 (right). These particles were analyzed by EDX spectroscopy, and we believe that these are the residues of $LiPF_6$ or its decomposition products. Thus, we can conclude that the washing condition should be optimized to ensure full removal of old electrolyte.

To optimize the washing conditions, we first developed a methodology for analysis of lithium compounds, which are washed from the electrodes or cells.

The kinetics of electrolyte washing was analyzed by ICP MS analysis of the probes, which were obtained by bubbling the exhaust of the high-pressure experimental setup through deionized water. For this purpose, the high-pressure experimental setup developed at the previous project stage was upgraded by adding one more high-pressure reactor for the co-solvent. The scheme is shown in Figure 5. Supercritical CO_2 flows from pressure generator (2) firstly to the reactor I (3), which contains an excess of co-solvent for washing. Then supercritical fluid consisting of CO_2 and co-solvent, which amount is determined by its solubility in $scCO_2$ at given pressure and temperature, flows to the reactor II (4), in which electrolyte droplet, or electrode or cell is located. The object under study is flushed with the fluid going further to back-pressure regulator (5) and the to the flask with deionized water where the probe is collected. We found that part of ionic compounds precipitates in the capillaries right after decompression in the BPR. To avoid the underestimation of the washed lithium amounts we developed a three-step procedure of probe collection, which is described below.

Step 1 - Preliminary washing with water.

10 ml of deionized water was placed in reactor II, reactor I was disconnected from the system and cleaned manually with deionized water. The entire experimental setup was purged with CO_2 for 10 minutes, and as a result water from reactor II entered the BPR and washed all the internal capillaries from possible residual lithium compounds. At the BPR outlet, water and CO_2 flowed into flasks with deionized water. Each iteration, a change in the volume of water in the flask was recorded. In each experiment, 5-7 washing operations described above were performed. The dependencies of lithium concentration with the probes on the number of wash cycles always represented by an asymptotically decreasing curve. The approximate background level (the lithium concentration determined by ICP MS, which is due to contamination of the system with lithium) was calculated based on such dependencies (see Figure 9).

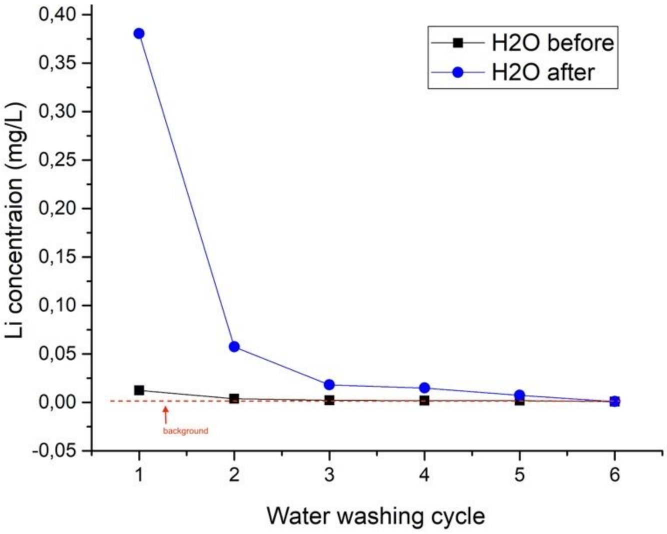

Figure 9 Lithium concentration in the exhaust from high pressure system during water washing cycles before and after SCF washing of battery components.

Step 2 - Washing of the samples with supercritical carbon dioxide with a co-solvent

The samples were placed in reactor II, and co-solvent was poured in reactor I. The entire experimental setup was purged with CO_2 for 20 minutes, and as a result CO_2 was fed into reactor I, mixed with co-solvent, got into reactor II, mixed (dissolved) with electrolyte and got into the flask with water through the BPR at the BPR outlet. Each iteration, a change in the volume of water in the flask was recorded. After 20 minutes of washing, the flask with water at the BPR outlet was replaced. The total number of such washing cycles was 6, which is equivalent to 2 hours of washing. To calculate the total amount of lithium washed during these cycles, the background signal was subtracted from the concentration value for each washing cycle. The total amount of lithium was obtained by summation of the results for each cycle.

Step 3 - Final washing with water

This step was necessary for leaching lithium remaining on the capillaries and the BPR needle after previous step. The whole process was similar to preliminary washing with water. 10 ml of distilled water was placed in reactor II, reactor I was disconnected from the system and cleaned manually with distilled water. The entire experimental setup was purged with CO_2 for 10 minutes, and as a resulting water from reactor II entered the BPR and washed all the internal capillaries with possible residual lithium. At the BPR outlet, water and CO_2 flowed into flasks with water. Each cycle, a change in the volume of water in the flask was recorded. In each experiment, 5 described washing cycles were performed. Amount of lithium washed on this step was calculated by the same procedure as for the step 2. The amount of lithium washed in steps 2 and 3 were then summed.

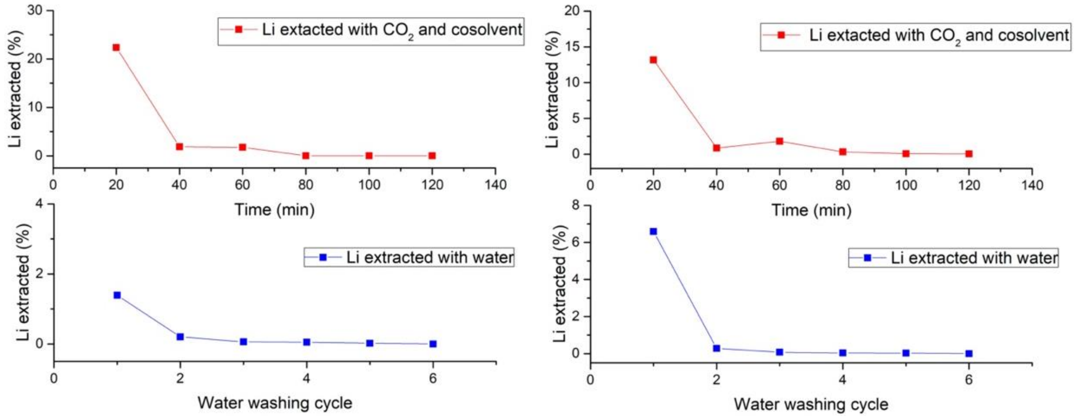

Figure 10 The kinetics of lithium extraction from the high-pressure reactor. Left panel shows the results for acetonitrile as a co-solvent, right – for EC:DMC mixture.

We compared washing with MeCN and with EC:DMC mixture as a co-solvents. 70 μl of electrolyte (which contains 0.49 mg of Li) was poured into reactor II, and 50 ml of co-solvent was poured into reactor I.

During the experiment time (2 hours) 44 ml of MeCN was spent, while in the experiment with EC:DMC co-solvent – only 30 ml. At the same time MeCN- and EC:DMC-assisted washing resulted in nearly the same percent of lithium, which was extracted – 28 and 23%, respectively. At the same time, as can be seen in Figure 10, the effective washing lasts for only first 40 minutes and seems to be controlled by the amount of available co-solvent. It can be also indirectly proved by similar experiment with a lack of co-solvent, which is illustrated in Figure 11 for MeCN. In this case we used only 1 ml of co-solvent, which resulted in full consumption of MeCN and extraction of only 0.9% of lithium. We can suppose, that using a continuous excess of co-solvent, e.g. acetonitrile, can enable and effective washing of all electrolyte (and possible part of SEI) from the spent LIBs.

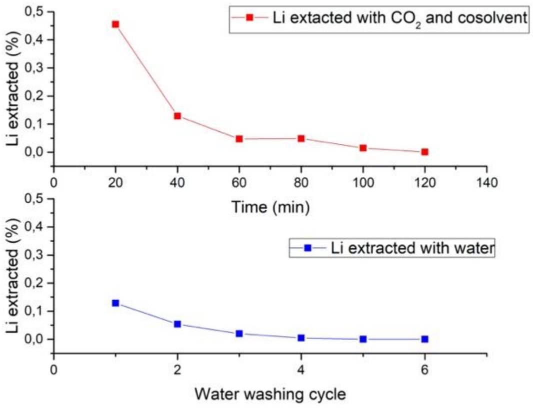

Figure 11 The kinetics of lithium extraction from the high-pressure reactor. Extraction was performed by $scCO_2$ – MeCN mixture. Only 1 ml of acetonitrile was available in the system.

Thus, we demonstrated that the old electrolyte can be washed out using the supercritical fluids. We further checked whether the cell performance would be affected by treatment in $scCO_2$. For this purpose, we cycled 80 mAh pouch cells (graphite vs. NMC chemistry), then the Al-laminated foil was cut on the one side of the cell. The cell was washed by supercritical fluid at 60℃ and 300 bar for 2 hours, then transferred to glove box, refilled with electrolyte, resealed and tested again. Control experiments were also performed to check the effect of fresh electrolyte addition without washing.

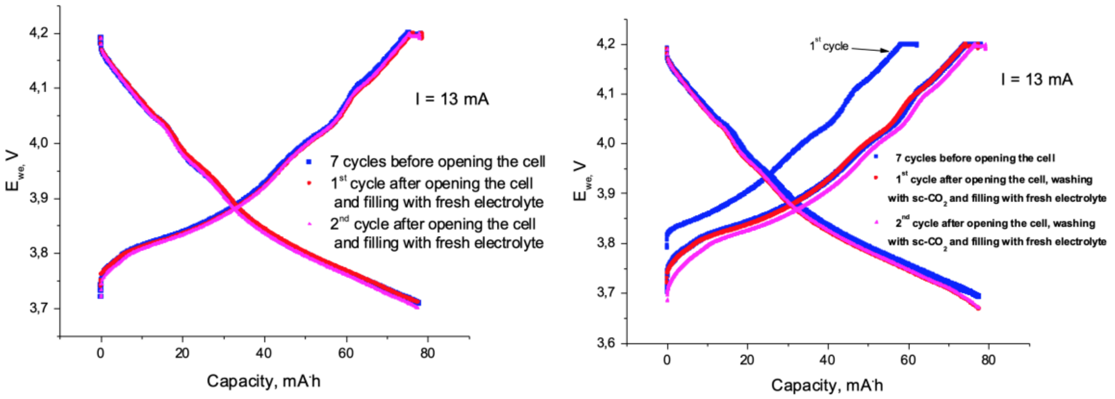

Figure 12 Charge-discharge voltage profiles for two 80 mAh pouch cells recorded before and after cutting of the pouch, filling fresh electrolyte and resealing (on the left, control experiment) or $scCO_2$-washing and further filling/resealing (right). Charge was performed in CC/CV mode at 13 mA and then at 4.2 V. Discharge – at 13 mA (C/5).

As seen in Figure 12 the LIB pouch cells are fully operative after treatment with SCF, and the procedure of cell unsealing, filling (or refilling) with electrolyte and resealing doesn't affect its performance.

The negative electrodes from the cycled pouch cells were also tested in half-cells vs. metallic lithium (coin cells were used). The results are shown in Figure 13.

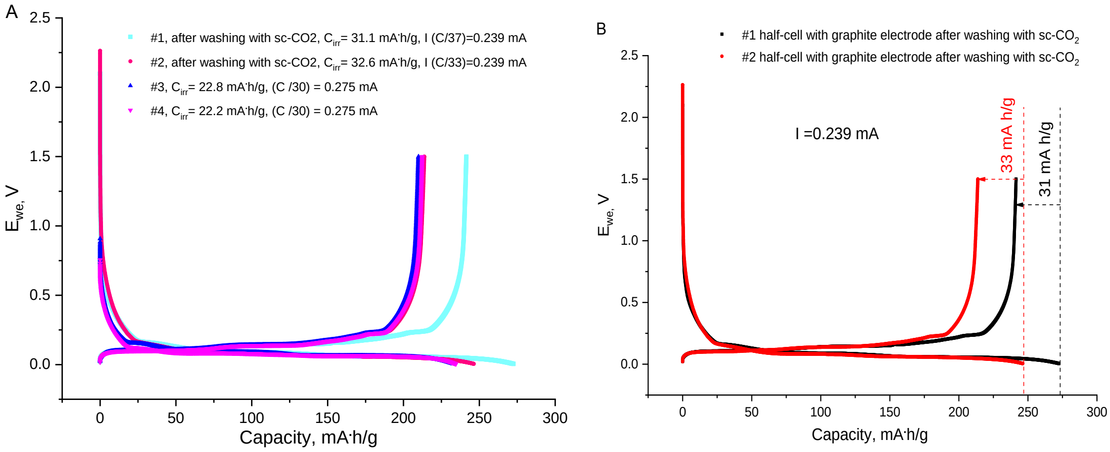

Figure 13 (A) Discharge-charge voltage profiles for half-cells (graphite vs. lithium). Graphite electrode were cut from disassembled and cycled pouch cells. Coin cells #1 and 2 were assembled using the electrodes, which were washed by SCF after cutting, while cells #3 and 4 were assembled using the electrodes, which were not washed. (B) Discharge-charge profiles for half-cells #1 and #2 with graphite electrodes washed with SCF after cutting. Increased irreversible capacity is illustrated by arrows and dash lines.

Although one of the electrodes, which was washed by SCF, demonstrated a little higher capacity than those, which were not washed, it turned out that it was cycled at slightly lower current density. So, it cannot be a direct evidence of any capacity improvement, which in fact was not expected unless we use a special “recovery” electrolyte, which shall change the old electrolyte. Another observation seems, however, reliable – both electrodes after washing demonstrated increased irreversible capacity with no loss of specific capacity. It may indirectly indicate that SEI is at least partially removed from the graphite.

Searching and testing the electrolytes for lithium inventory refilling

Lithium inventory refilling requires some sacrificial electrolyte, which anion would be oxidized along with lithium intercalation into graphite. In standard LIB electrolytes during intercalation into graphite oxidation proceeds with d-metals of cathode material, from which lithium ions are extracted. In degraded battery, however, the amount of lithium in cathode material is lower than it should be, thus extraction of all available lithium ions accompanied by oxidation of all available d-metal ions in structure won't be enough for compensation of capacity loss.

At the last project stage, backed by literature survey we selected few potential electrolyte salts, which have anions capable of oxidizing at relatively low voltages. They are summarized in **Table 1**.

Table 1 Summary of that lithium salts, which can be suggested as an electrolyte for refilling lithium inventory.

Salt	Oxidation mechanism	Reduction mechanism	Ref.
$Li_2C_2O_4$	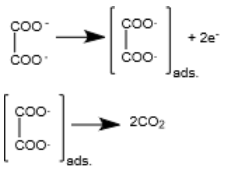	$Li^+ + C_6 + e^- \rightarrow LiC_6$	[7]
	$C_2O_4^{2-} - e^- \rightarrow C_2O_4^{-}\cdot$ $C_2O_4^{-}\cdot \rightarrow CO_2 + CO_2^{-}\cdot$ $CO_2^{-}\cdot - e^- \rightarrow C_2O_4 \rightarrow 2CO_2$ $CO_2^{-}\cdot - e^- \rightarrow CO_2$	$Li^+ + C_6 + e^- \rightarrow LiC_6$	[8]
CH_3COOLi	$2CH3COO^- \rightarrow 2CO2 + C2H6 + 2e^-$	$Li^+ + C_6 + e^- \rightarrow LiC_6$	[9]
$LiNO_3$	$NO_3^- - e^- \rightarrow NO_3\cdot$ $2NO_3\cdot \rightarrow N_2O_6$ $N_2O_6 \rightarrow N_2O_5 + ½ O_2$	$Li^+ + C_6 + e^- \rightarrow LiC_6$	[10]
	$NO_3^- \leftrightarrow NO_2 + ½ O_2 + e^-$ or $2NO_3^- \leftrightarrow N_2O_5 + \frac{1}{2} O_2 + 2e^-$	$Li^+ + C_6 + e^- \rightarrow LiC_6$	[11]

At this stage we tested these salts preparing the electrolyte solutions with it. EC:DMC mixture was used as a solvent. Unfortunately, we faced a problem of a low solubility of oxalate and acetate and, as a consequence, of low electrolyte conductivity. Lithium nitrate demonstrates better solubility, however, we prepared 0.03 M solution for comparison with other salts. To increase the electrolyte conductivity in our model studies, we also compared the data for low-concentration solutions with the electrolytes containing the considered salts and TBAP as a supporting electrolyte.

The EIS data recorded in three-electrode glass cell and represented in Nyquist coordinates are shown in Figure 14, Figure 15 and Figure 16 for saturated lithium oxalate, saturate lithium acetate and 0.03 M lithium nitrate solution in EC:DMC, respectively. It can be easily seen that internal resistance falls down by few orders of magnitude when TBAP is added that is a consequence of low concentration. It's also worth noticing that both pure saturated solutions of $Li_2C_2O_4$ and CH_3COOLi demonstrate the total cell impedance of hundreds kOhms, while even 0.03 M of $LiNO_3$ is enough to get few kOhms. It may indicate that either solubility is much lower than ~0.01 M or/and dissociation constant for these salts is quite low.

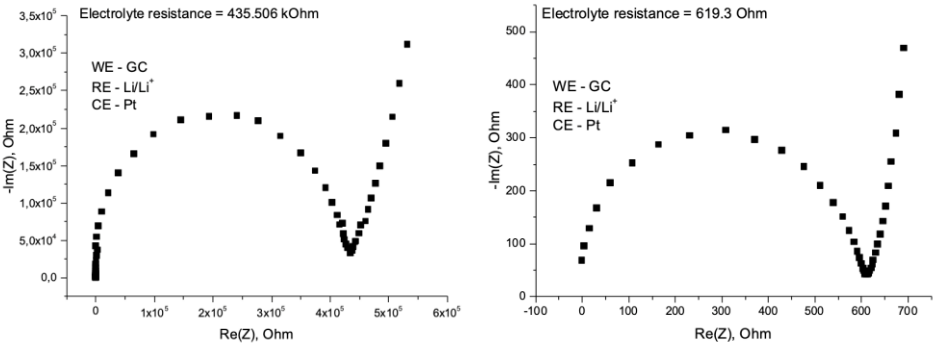

Figure 14 Electrochemical impedance spectra for saturated solution of $Li_2C_2O_4$ in EC:DMC mixture (left) and for the same solution with 0.1 M TBAP added (right).

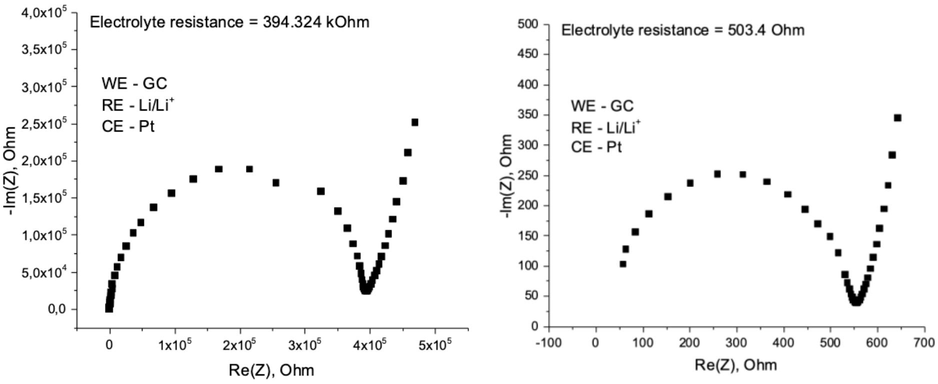

Figure 15 Electrochemical impedance spectra for saturated solution of CH_3COOLi in EC:DMC mixture (left) and for the same solution with 0.1 M TBAP added (right).

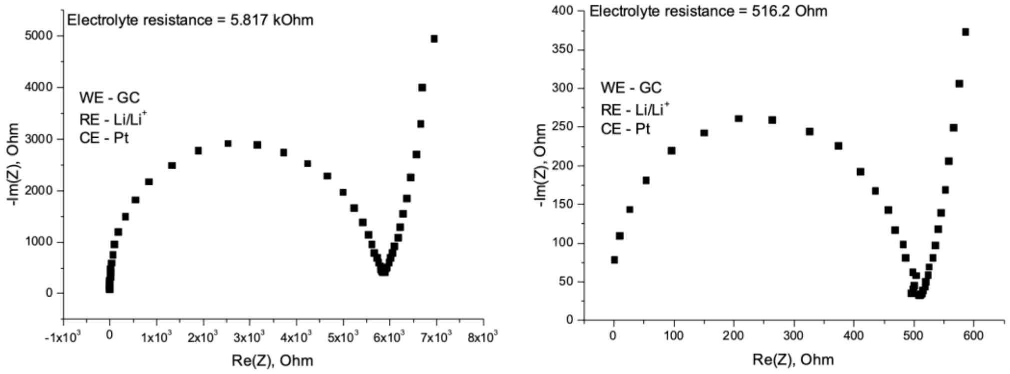

Figure 16 Electrochemical impedance spectra for 0.03 M solution of $LiNO_3$ in EC:DMC mixture (left) and for the same solution with 0.1 M TBAP added (right).

We further performed CVA analysis of the salts in order to estimate the ability to oxidize the anions at lower potentials that oxidation of solvent starts. In spite of high resistivity of solution with no TBAP added it was possible to obtain voltammograms, which are shown in Figure 17. We see oxidation onset before solvent oxidation for all the salts indication the possibility to use it for "recovery" electrolytes.

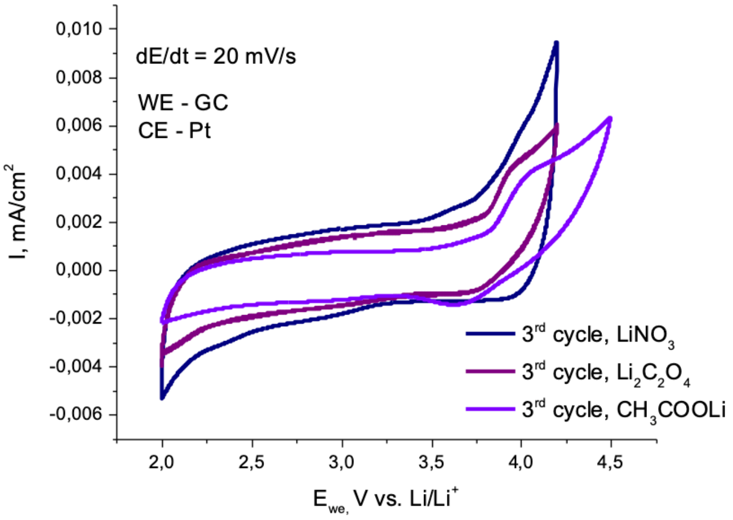

Figure 17 CVA curves for sat. $Li_2C_2O_4$, sat. CH_3COOLi and 0.03 M $LiNO_3$ in EC:DMC.

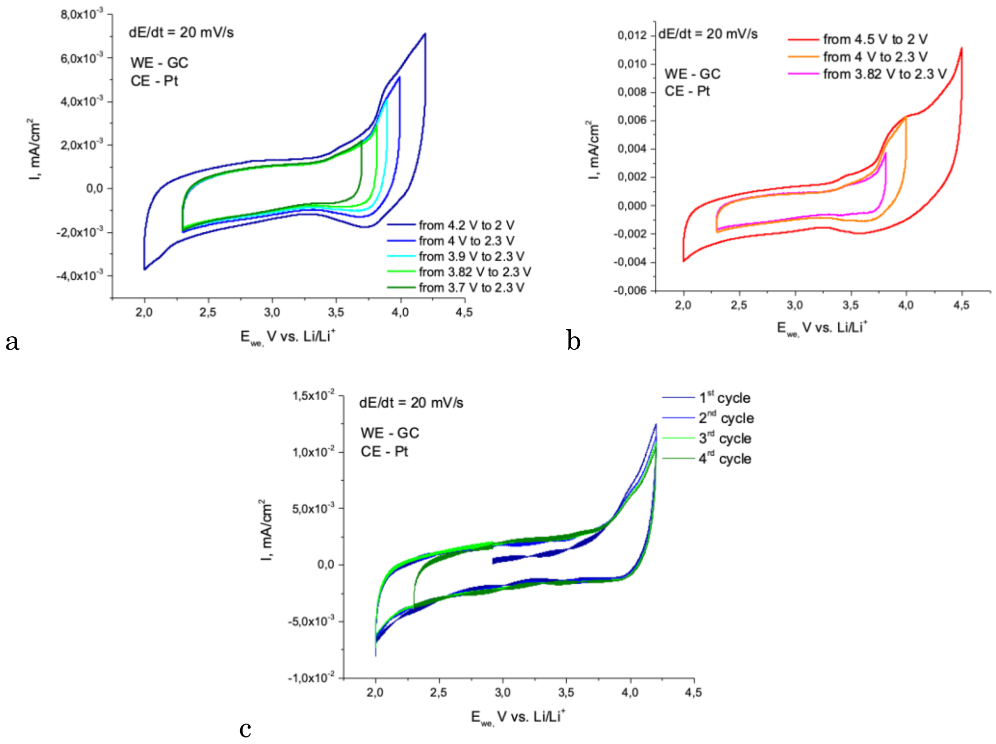

Figure 18 CVA curves for (a) sat. $Li_2C_2O_4$, (b) sat. CH_3COOLi and (c) 0.03 M $LiNO_3$ with 0.1 M TBAP addition in EC:DMC.

In some case (lithium acetate and oxalate) the reverse reduction peak appears most probably due to reduction of oxidation products. To prove that the upper potential limit was varied for these salts (see Figure 18a, b), in which we see that reduction peak is absent unless a significant amount of charge were spent for oxidation on the semicycle preceding the reduction.

Lithium nitrate showed no reduction peaks, however, it can be explained by formation of non-soluble oxidation products. As well, higher charging currents was observed for lithium nitrate that can be connected with higher concentration but it requires further testing. Unfortunately, due to low concentration the attempts to implement Li^+ intercalation into graphite using acetate or oxalate electrolyte and lithium-free counter electrode was unsuccessful. $LiNO_3$ being much more soluble still gives a hope that we can intercalate lithium into graphite preforming anion oxidation at counter electrode.

Possible approaches for All-Solid-State Battery regeneration

Interfacial problems caused by significant volume change during charge/discharge are considered to be one of the major issues in development of all solid-state batteries. Such volume changes lead to cracking of both active materials and solid electrolyte and eventual loss of contact between the phases which results in dramatic increase of interfacial resistance and corresponding overvoltage increase.

One of the possible approaches to restore the damaged interphase is to heat one of the phases above melting temperature. While this approach is not viable for ceramic electrolytes due to extremely high melting temperatures it may work for polymer-based systems. However, even for polymer systems one should find the material with an appropriate melting temperature: not too low to assure solid state of the electrolyte during battery operation and not too high to minimize negative effects of heating on other elements of the battery. It would be great to have an instrument to control the melting temperature of the polymer electrolyte: to decrease it before such restoration procedure and increase back to its initial value after the interphase is restored. It could be done by addition of plasticizers into the electrolyte which can be easily extracted after the procedure. Certain supercritical fluids such as CO_2 or some short fluorocarbons can be used as such plasticizers. The melting temperature in this case can be changed by controlling the pressure. Indeed, it is known that polyethyleneoxide (PEO), which is one of the most widely studied materials for polymer ASSB [12], dissolves significant amounts of CO_2 (up to 30 wt. %) at pressures between 100 and 150 bar [13,14], which results in a pronounced decrease of melting temperature (of about 10-15 °C in a range 40-60 °C depending on PEO molecular weight) [13] and almost 10-fold decrease in viscosity (Figure 19)[15]. For lower molecular weight PEO the viscosity drops down to values only 2-3 times higher than that of water at normal conditions. For higher molecular weights the decrease of viscosity may be less pronounced due to entanglements of polymer chains but should take place as well.

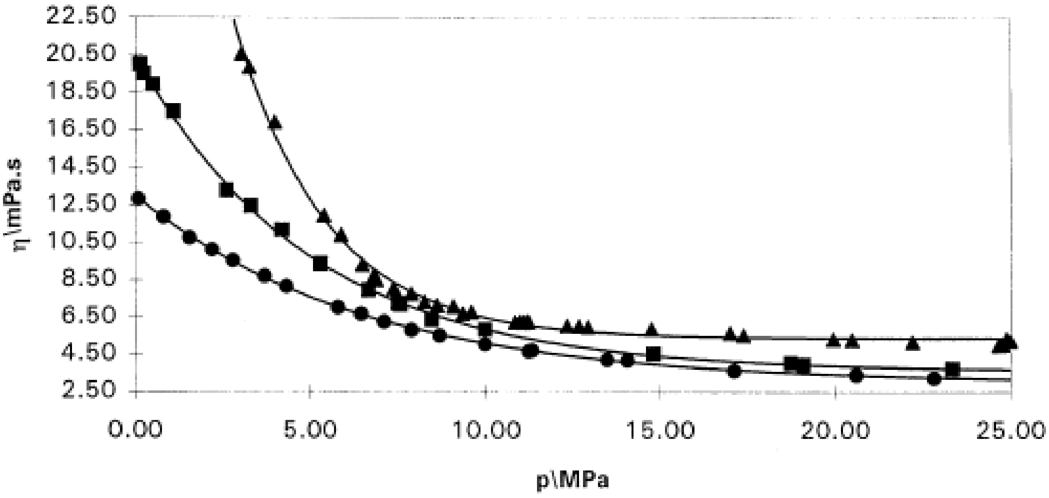

Figure 19. Plot of CO_2-saturated PEG-400 Viscosity vs CO_2 pressure at 313.25 K (triangles), 332.89 K (squares) and 347.77 K (circles). Ref. [15]

This fact as well as the fact that the CO_2 exposition is not harmful for Li-ion battery components and batteries after such exposition show high reproducible performance, allow one to propose the concept of switchable solid/flow battery device shown in Figure 20.

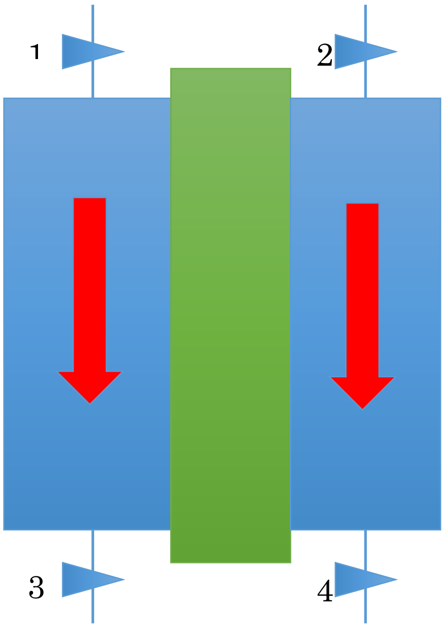

Figure 20. The principal scheme of switchable solid/flow battery device. The electrode materials are liquefied in supercritical fluid environment at elevated pressures and temperatures and can be pumped out through the valves 3 and 4. Fresh electrode materials can be pumped in though the valves 1-2. Red arrows illustrate the flow of electrode materials.

The idea is that the electrolyte can be turned into liquid state upon exposition to supercritical fluid at elevated pressure (about 100 bar) and temperature (about 60°C or slightly higher) using the valves 1-4 shown in Figure 20. It provides three very important advantages:

1. The battery could be recharged quickly by pumping out the discharged anode and cathode materials in liquid state and filling electrode compartments with charged electrolytes trough the valves 1-4.
2. Old degraded materials covered with SEI could be removed from the battery and can be further processed and restored separately.
3. The interphase between electrolyte and active materials with better contact and lower impedance is formed since the electrolyte is in a liquid state.

After the exchange of electrode materials the pressure is released, the valves are closed and the system goes back to solid state. One gets charged battery ready for operation.
The previous experience of the project group in making PEO-based ASSB which have shown reproducible performance (Figure 21) as well as our experience in working with

supercritical fluids and the results of the previous stages of the project show that this concept may be viable.

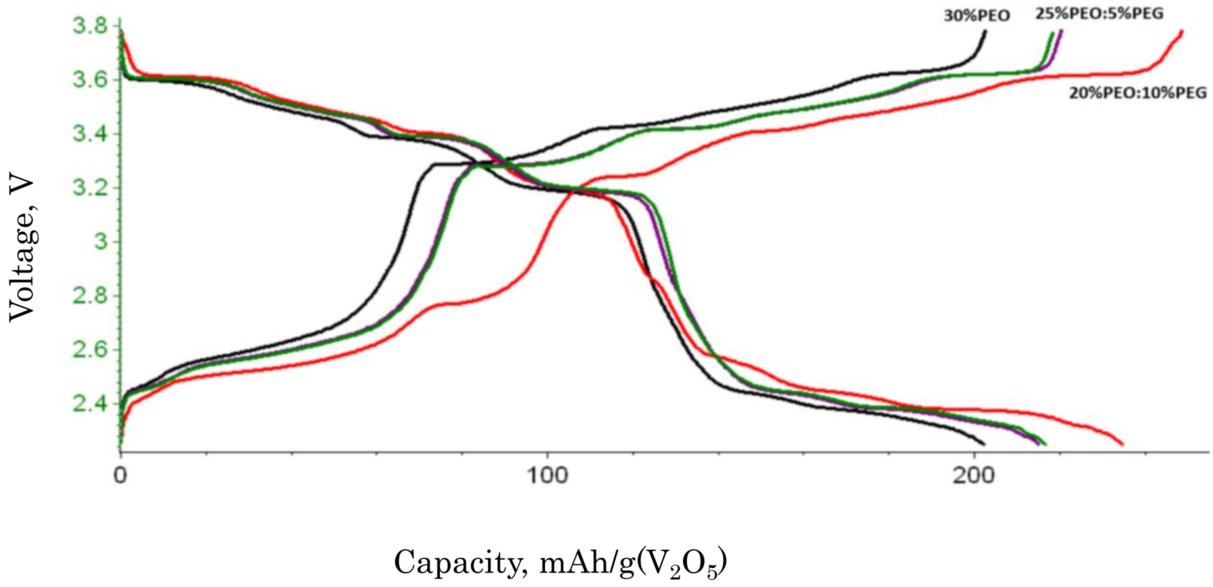

Figure 21. The performance of Li-V_2O_5 ASSB with PEO based electrolytes of different composition tested by the project team.

The proposed concept could be checked using simple PEO-based ASSB system.

The brief research plan is as follows:

- Studying phase behavior of PEO mixed with Li-salts in supercritical fluid environment.
- Studying phase behavior of PEO based electrolytes filled with active anode and cathode materials in supercritical fluid environment.
- If the viscosity is not very high in the next step we are going to design high pressure electrochemical half-cells to try replacing anode and cathode materials separately followed by electrochemical characterization in the same cell.

If the concept is viable the electrolyte material properties could be tuned by switching from PEO to other polymer host materials [12] and varying the composition of the electrodes. Probably the other supercritical solvents with higher dielectric constant and still low critical pressures and temperatures such as trifluoromethane [16] and other fluorocarbons could be checked as well.

Conclusions

- **Treatment by scCO2 at temperature up to 60°C and pressures up to 300 bar does not damage the Li-ion pouch cells, which remain fully operational** after washing and further refilling with a fresh electrolyte and resealing, anode microstructure remains stable as confirmed by SEM. At the same time such treatment enables full removal of aged (old) electrolyte from the cells as confirmed by mass-spectrometry studies on model systems.
- **As expected, scCO2 treatment combined with refilling of the cells with conventional electrolyte does not lead to the cell capacity improvement**. However, we found that the anode specific capacity after SCF-washing of the electrodes doesn't decrease, while the irreversible capacity appears that indicate at least partial removal of SEI. As the total cell capacity remains stable after washing, and at the same time the separately tested anode also shows stable capacity we can deduct that the cathode capacity is also maintained upon washing.
- For capacity recovery the cells washed by SCF should be refilled with a special "recovery" electrolyte (i.e. electrolyte with additional Li salt, which anion easily decompose with the formation of gaseous products). During this project stage the search for such electrolyte based on previous literature survey was performed. **Unfortunately, a proper "recovery electrolyte" was not found as the salts, which has been believed to be suitable, were found to be poorly soluble in alkyl-carbonates.**

Finally, at the moment the proposed approach was not demonstrated to improve cell capacity and the bottleneck was found to be low solubility of the salts suggested for "recovery electrolyte" for lithium inventory refilling. We hope to resolve this issue by continuing the search for other salts.

Challenges for the future

- Successful intercalation of lithium into graphite using “recovery” electrolyte and lithium-free counter electrode was not demonstrated, although the selected salts for “recovery” electrolyte demonstrated the potential ability to perform the task. Most probably, the problem is caused by very low solubility, leaving only lithium nitrate as a candidate for further attempts. Lithium nitrate-based “recovery electrolytes” should be more thoroughly studied.
- Design of the pouch cells, which can be sealed/unsealed multiple times for recovery experiments.
- Evaluating of possible designs of ASSB capable for recovery after degradation
    - Studying phase behavior of PEO mixed with Li-salts in supercritical fluid environment.
    - Studying phase behavior of PEO based electrolytes filled with active anode and cathode materials in supercritical fluid environment.
    - Designing high pressure electrochemical half-cells to try replacing anode and cathode materials separately followed by electrochemical characterization in the same cell.

References

1. Xu J., Thomas H. R., Francis R. W., Lum K. R., Wang J., Liang B. A review of processes and technologies for the recycling of lithium-ion secondary batteries // Journal of Power Sources – 2008 – vol. 177 (2) – pp. 512-527
2. Zeng X., Li J., Singh N. Recycling of spent lithium-ion battery: a critical review // Critical Reviews in Environmental Science and Technology – 2014 – vol. 44 (10) – pp. 1129-1165
3. Ramoni M. O., Zhang H. C. End-of-life (EOL) issues and options for electric vehicle batteries // Clean Technologies and Environmental Policy – 2013 – vol. 15 (6) – pp. 881-891
4. Ordoñez J., Gago E. J., Girard A. Processes and technologies for the recycling and recovery of spent lithium-ion batteries // Renewable and Sustainable Energy Reviews – 2016 – vol. 60 – pp. 195-205
5. Birkl C. R., Roberts M. R., McTurk E., Bruce P. G., Howey D. A. Degradation diagnostics for lithium ion cells // Journal of Power Sources – 2017 – vol. 341 – pp. 373-386
6. B. Rumberg, B. Epding, I. Stradtmann, A. Kwade, Identification of Li ion battery cell aging mechanisms by half-cell and full-cell open-circuit-voltage characteristic analysis, Journal of Energy Storage. 25 (2019) 100890. doi:10.1016/j.est.2019.100890.
7. Jacobsen E., Sawyer D.T. Electrochemical oxidation of oxalate ion in dimethylsulfoxide at a golden electrode // Journal of Electroanalytical Chemistry and Interfacial Electrochemistry – 1967 – vol. 16 – pp. 361-374
8. Chang M.M., Saji T., Bard A.J. Electrochemical oxidation of oxalate ion in the presence of luminescers in acetonitrile solutions // Journal of the American Chemical Society – 1977 – vol. 99 – pp. 5399-5403
9. Ross S.D., Finkelstein M., Petersen R.C. The electrochemical oxidation of acetic acid in the presence of aromatic hydrocarbons // Journal of the American Chemical Society – 1964 – vol. 86 – pp. 4139–4143
10. Rao R. R., Milliken S.B., Robinson S. L., Mann C. K. Anodic oxidation of lithium, cadmium, silver, and tetra-n-butylammonium nitrates // Analytical Chemistry – 1970 – vol. 42 – pp. 1076–1080

11. Mishima H., Iwasita T., Macagno V. A., Giordano M. C. The electrochemical oxidation of nitrate ion on platinum from silver nitrate in acetonitrile solutions – I. Kinetic analysis // Elecfrochimica Acta – 1973 – vol. 18 – pp. 287–292
12. J. Mindemark, M.J. Lacey, T. Bowden, D. Brandell, Beyond PEO—Alternative host materials for Li+-conducting solid polymer electrolytes, Prog. Polym. Sci. 81 (2018) 114–143. doi:10.1016/j.progpolymsci.2017.12.004.
13. E. Weidner, V. Wiesmet, Ž. Knez, M. Škerget, Phase equilibrium (solid-liquid-gas) in polyethyleneglycol-carbon dioxide systems, J. Supercrit. Fluids. 10 (1997) 139–147. doi:10.1016/S0896-8446(97)00016-8.
14. D.J. Heldebrant, P.G. Jessop, Liquid poly(ethylene glycol) and supercritical carbon dioxide: A benign biphasic solvent system for use and recycling of homogeneous catalysts, J. Am. Chem. Soc. 125 (2003) 5600–5601. doi:10.1021/ja029131l.
15. D. Gourgouillon, H.M.N.T. Avelino, J.M.N.A. Fareleira, M. Nunes da Ponte, Simultaneous viscosity and density measurement of supercritical CO2-saturated PEG 400, J. Supercrit. Fluids. 13 (1998) 177–185. doi:10.1016/S0896-8446(98)00050-3.
16. P.N. Bartlett, D.A. Cook, M.W. George, A.L. Hector, J. Ke, W. Levason, G. Reid, D.C. Smith, W. Zhang, Electrodeposition from supercritical fluids, Phys. Chem. Chem. Phys. 16 (2014) 9202–9219. doi:10.1039/c3cp54955k.